

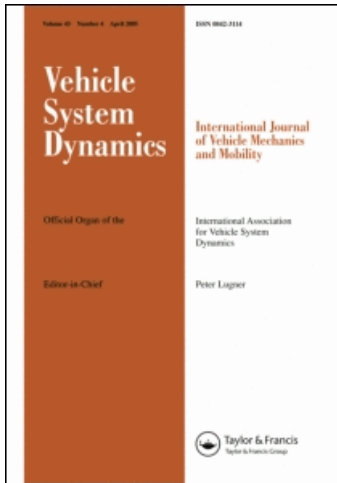
This article was downloaded by: [Politecnico di Milano]

On: 2 December 2010

Access details: Access Details: [subscription number 922320753]

Publisher Taylor & Francis

Informa Ltd Registered in England and Wales Registered Number: 1072954 Registered office: Mortimer House, 37-41 Mortimer Street, London W1T 3JH, UK



Vehicle System Dynamics

Publication details, including instructions for authors and subscription information:

<http://www.informaworld.com/smpp/title~content=t713659010>

Performance analysis of semi-active suspensions with control of variable damping and stiffness

Cristiano Spelta^a; Fabio Previdi^a; Sergio M. Savaresi^b; Paolo Bolzern^b; Maurizio Cutini; Carlo Bisaglia; Simone A. Bertinotti

^a Dipartimento di Ingegneria dell'Informazione e Metodi Matematici, Università degli Studi di Bergamo, Dalmine, BG, Italy ^b Dipartimento di Elettronica e Informazione, Politecnico di Milano, Milano, Italy

First published on: 29 July 2010

To cite this Article Spelta, Cristiano , Previdi, Fabio , Savaresi, Sergio M. , Bolzern, Paolo , Cutini, Maurizio , Bisaglia, Carlo and Bertinotti, Simone A.(2010) 'Performance analysis of semi-active suspensions with control of variable damping and stiffness', Vehicle System Dynamics,, First published on: 29 July 2010 (iFirst)

To link to this Article: DOI: 10.1080/00423110903410526

URL: <http://dx.doi.org/10.1080/00423110903410526>

PLEASE SCROLL DOWN FOR ARTICLE

Full terms and conditions of use: <http://www.informaworld.com/terms-and-conditions-of-access.pdf>

This article may be used for research, teaching and private study purposes. Any substantial or systematic reproduction, re-distribution, re-selling, loan or sub-licensing, systematic supply or distribution in any form to anyone is expressly forbidden.

The publisher does not give any warranty express or implied or make any representation that the contents will be complete or accurate or up to date. The accuracy of any instructions, formulae and drug doses should be independently verified with primary sources. The publisher shall not be liable for any loss, actions, claims, proceedings, demand or costs or damages whatsoever or howsoever caused arising directly or indirectly in connection with or arising out of the use of this material.

Performance analysis of semi-active suspensions with control of variable damping and stiffness

Cristiano Spelta^{a*}, Fabio Previdi^a, Sergio M. Savaresi^b, Paolo Bolzern^b, Maurizio Cutini^c, Carlo Bisaglia^c and Simone A. Bertinotti^c

^aDipartimento di Ingegneria dell'Informazione e Metodi Matematici, Università degli Studi di Bergamo, viale Marconi 5, 24044 Dalmine (BG), Italy; ^bDipartimento di Elettronica e Informazione, Politecnico di Milano, Piazza L. da Vinci, 32, 20133 Milano, Italy; ^cCRA-ING, Laboratorio di Treviglio via Milano 43, 24043 Treviglio (BG), Italy

(Received 10 July 2009; final version received 5 October 2009)

The problem considered in this paper is the study and the control strategy design of semi-active suspensions, featuring the regulation of both damping and stiffness. The first contribution of this paper is the introduction and the analysis of two architectures based on the use of only controllable dampers, which make possible the emulation of an ideal suspension with controllable-damping-and-stiffness. This work presents an evaluation of the performances and drawbacks achieved by such suspension architectures, also in a nonlinear setting (explicitly taking into account the stroke limits of the suspension). This paper then proposes a new comfort-oriented variable-damping-and-stiffness control algorithm, named stroke–speed–threshold–stiffness–control, which overcomes the critical trade-off between the choice of the stiffness coefficient and the end-stop hitting. The use of a variable-damping-and-stiffness suspension, together with this algorithm, provides a significant improvement of the comfort performances, if compared with traditional passive suspensions and with more classical variable-damping semi-active suspensions.

Keywords: semi-active suspensions; damping control; stiffness control; nonlinear systems

1. Introduction

Among the many different types of controlled suspensions (see, e.g. [1] for a detailed classification), semi-active suspensions have received a lot of attention in the last two decades, since they provide the best compromise between cost (energy consumption and actuators/sensors hardware) and performance [1–20].

A classical semi-active suspension is characterised by the closed-loop regulation of the damping coefficient; the electronic modulation of the damping coefficient is obtained with magneto-rheological, electro-rheological, or electro-hydraulic technologies. In the last years, variable-damping semi-active suspensions have had a large growth, and today they are employed over a wide range of application domains: road vehicles suspensions,

*Corresponding author. Email: cristiano.spelta@unibg.it

cabin suspensions in trucks or agricultural tractors, seat suspensions, lateral suspensions in high-speed trains, etc. [1,11,13–15,21–51].

The research activity in this field is carried out along two mainstreams: the development of new technologies for semi-active actuation systems [6,52–54], and the development of new control algorithms and control strategies for such systems [19,43–45,55–58]. This paper belongs to both of these research areas: the application of controllable shock absorbers in the suspension system architecture capable of modulating both the damping and the equivalent stiffness coefficients is presented; based on this kind of system, a new control algorithm is also developed and discussed.

While the modulation of the damping coefficient is commonly used and can be easily obtained with different technologies, the control of the spring stiffness is a much more subtle and elusive problem. It is well known that classical load-levelling or slow-active suspensions based on hydro-pneumatic or pneumatic technologies are subject to spring-stiffness variations, but the stiffness change is more a side-effect than a real control variable [9,35,55]. A variation of the spring coefficient can be achieved in active suspension (see, e.g. [11,59,60] and references cited therein). However, the goal of this work is to devise a genuine variable-damping-and-stiffness suspension system in a semi-active framework: with only controllable shock-absorbers with a fast switching of damping. Thus, the resulting system is characterised by the so-called ‘passivity constraint’: no or relatively little power is injected into the suspension system [1].

The research area of variable-damping-and-stiffness suspensions in a semi-active framework is still largely unexplored; a few works have been proposed on this topic [34,35], mainly focused on the description of variable-damping architectures capable of approximating an ideal variable-stiffness suspension.

This work contains (to the best of our knowledge) innovative contributions in many directions:

- Two different suspension architectures are presented, capable of reproducing a variable-damping-and-stiffness suspension system, based on the contributions in [34,35].
- A detailed analysis on the advantages and trade-offs of the two variable-damping-and-stiffness suspension systems is developed. Obviously enough, if we consider the comfort objective for variable-damping semi-active suspension [12,19,58] during a standard working condition, a ‘soft’ spring ensures the best performance. On the other hand, this setting requires a wider stroke travel, so if the road disturbance is particularly exciting, the end-stops can be hit and the performance decreases dramatically. On the contrary, an ‘hard’ spring decreases the chance of end-stop hitting, but the filtering capabilities of the suspension are poor. A control of the stiffness is able to overcome such a trade-off. To this purpose, an optimality analysis is performed using the framework of the optimal predictive control, based on the assumption of full knowledge of the road disturbance [3]. This result provides a numerical estimation of the performance limits of a suspension with variable damping and stiffness.
- An innovative control strategy suited to variable-damping-and-stiffness suspensions is proposed. The algorithm presented herein is named *stroke-speed-threshold-stiffness-control* (SSTSC): it is based on the recently developed mixed sky-hook (SH)–Acceleration Driven Damping (ADD) rationale [14] for the control of variable-damping suspensions.

The work presented herein is focused on a single-suspension of a road vehicle (namely a two-mass quarter-car suspension system). The control objective is the minimisation of the vertical acceleration of the vehicle; this is the so-called ‘comfort-objective’. Most of the control strategies in the vast literature on semi-active suspension are designed according to this performance index, which has been also adopted by the ISO standard for the comfort

measure ([12,19,58] and reference cited therein). The design of an optimal comfort-oriented damping strategy has been an open issue for the last decades. Recent works presented damping rules for classical semi-active suspensions that can be considered optimal for comfort purposes [14,44,61].

In order to assess and to compare the closed-loop performance of the control strategy discussed in this paper, a numerical (simulation) approach, based on frequency-domain and time-domain analysis, is used. The performance assessment is made on streamlined models of the suspensions.

The outline of this paper is the following: in Section 2, the problem of approximating a semi-active suspension with variable damping and stiffness is discussed, and two architectures are introduced; in Section 3, the analysis of the suspension trade-off is described, and filtering limits of a variable-damping-and-stiffness suspensions are numerically evaluated, using a predictive optimal control approach; in Section 4, the SSTSC control algorithm is proposed and discussed. Section 5, ends the paper with some conclusive remarks.

2. Introducing stiffness control in a semi-active suspension

This section is devoted to the introduction and comparison of three quarter-car models as reported in Figure 1 (see for details, e.g. [1,9,12,42]). The first ideal suspension (IS) model describes an IS system with variable damping and stiffness. The other two architectures (activation damper system (ADS) and double suspension system (DSS) models), based on semi-active devices, can approximate the ideal system, and can be implemented in practice: these two architectures based on passive devices were previously introduced in [34,37] and herein generalised to a semi-active framework.

Quarter-car model of an IS with variable stiffness and damping:

$$\begin{cases} M\ddot{z}(t) = -c(t)(\dot{z}(t) - \dot{z}_t(t)) - k(t)(z(t) - z_t(t) - \Delta_s) - Mg \\ M\ddot{z}_t = +c(t)(\dot{z}(t) - \dot{z}_t(t)) + k(t)(z(t) - z_t(t) - \Delta_s) + \\ \quad -k_t(z_t(t) - z_r(t) - \Delta_t) - mg \\ \dot{c}(t) = -\beta c(t) + \beta c_{in}(t) \quad c_{min} \leq c_{in} \leq c_{max} \\ \dot{k}(t) = -\gamma k(t) + \gamma k_{in}(t) \quad k_{min} \leq k_{in}(t) \leq k_{max} \end{cases} \quad (1)$$

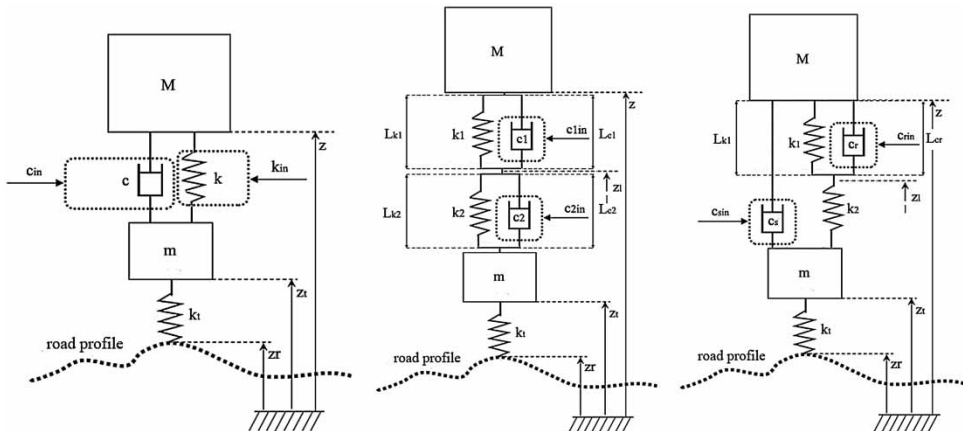


Figure 1. Quarter-car suspensions systems. From left to right: IS with variable damping and stiffness (IS); DSS; double springs with ADS.

Quarter-car model of a DSS:

$$\begin{cases} M\ddot{z}(t) = -k_1(z(t) - z_1(t) - \Delta_{s1}) - c_1(t)(\dot{z}(t) - \dot{z}_1(t)) - Mg \\ m\ddot{z}_t(t) = +k_2(z_1(t) - z_t(t) - \Delta_{s2}) + c_2(t)(\dot{z}_1(t) - \dot{z}_t(t)) + \\ \quad -k_t(z_t(t) - z_r(t) - \Delta_t) - mg \\ \dot{c}_1(t) = -\beta c_1(t) + \beta c_{1,in}(t) \quad c_{\min} = c_{1,in}(t) \leq c_{\max} \\ \dot{c}_2(t) = -\beta c_2(t) + \beta c_{2,in}(t) \quad c_{\min} = c_{2,in}(t) = c_{\max} \\ L_{k1} = L_{c1} \\ L_{k2} = L_{c2} \end{cases} \quad (2)$$

Quarter-car model of a suspension system with double spring and an ADS:

$$\begin{cases} M\ddot{z}(t) = -k_1(z(t) - z_1(t) - \Delta_{s1}) - c_r(t)(\dot{z}(t) - \dot{z}_1(t)) + \\ \quad -c_s(t)(\dot{z}(t) - \dot{z}_t(t)) - Mg \\ m\ddot{z}_t(t) = +k_2(z_1(t) - z_t(t) - \Delta_{s2}) + c_s(t)(\dot{z}(t) - \dot{z}_t(t)) + \\ \quad -k_t(z_t(t) - z_r(t) - \Delta_t) - mg \\ \dot{c}_s(t) = -\beta c_s(t) + \beta c_{s,in}(t) \quad c_{\min} = c_{s,in}(t) \leq c_{\max} \\ \dot{c}_r(t) = -\beta c_r(t) + \beta c_{r,in}(t) \quad c_{\min} = c_{r,in}(t) = c_{\max} \\ L_{k1} = L_{cr} \end{cases} \quad (3)$$

With reference to the diagrams in Figure 1, the symbols used in Equations (1)–(3) have the following meaning:

- M and m are the body mass (including the chassis, the engine, the passengers, etc) and the unsprung mass (tyre, wheel, brake caliper, suspension links, etc.), respectively.
- $z(t)$, $z_1(t)$, and $z_r(t)$ are the vertical positions of the body mass, the unsprung mass, and the road profile, respectively.
- $z_1(t)$ is the height of the intermediate link between the two springs in models (2) and (3).
- k_t and Δ_t are stiffness and the unloaded deflection of the tyre, respectively.
- $c(t)$ and $c_{in}(t)$ are the actual and requested damping of model (1), respectively. In the architectures (2) and (3) $c_j(t)$ and $c_{j,in}(t)$ stand for the actual and requested damping of the j th shock absorber, respectively.
- β is the modulation bandwidth of the controllable shock-absorbers. c_{\min} , c_{\max} is their controllability range.
- Considering model (1), $k(t)$ and $k_{in}(t)$ are the actual and requested spring coefficients, respectively. γ is the bandwidth of the controllable spring. The unloaded elongation is given by Δ_s which can assume two possible values according to $k_{in} \in \{k_{\min}, k_{\max}\}$. (k_{\min}, k_{\max}) is the controllability range of the spring.
- k_i and Δ_i are the stiffness coefficient and the unloaded deflection of the i th spring in Equations (2) and (3).
- $L_{c,i}$ and $L_{k,i}$ are to the elongation of the i th damper and i th spring, respectively, in Equations (2) and (3).

For simulation purposes, the following parameter values are used throughout the paper. $M = 400$ kg, $m = 50$ kg, $k_t = 250.000$ N/m, $k_{\min} = 5000$ N/m, $k_{\max} = 40,000$ N/m, $k_1 = 5700$ N/m, $k_2 = 40,000$ N/m, $c_{\min} = 150$ Ns/m, $c_{\max} = 3900$ Ns/m; $\gamma = \beta = 40 \cdot 2\pi$. The following nominal parameters are used: $c_{\text{nom}} = 1500$ Ns/m, $k_{\text{nom}} = 20,000$ N/m [19,44,62]. Note that the parameters are those of a standard European sedan (very similar to the one used in [19]). In order to explore the effect of the stiffness control, a relatively high

(k_2) and a relatively small (k_1) have been adopted. Those stiffness values may bring obnoxious movements of the suspensions, without an appropriate control of damping.

Models (1)–(3) are dynamical systems. They are constituted by a second-order differential equation for the body mass dynamics and a second-order differential equation for the unsprung mass vertical dynamics.

With reference to models (1)–(3), the following remarks are due:

- The models are nonlinear due to the fact that the damping coefficients $c(t)$ are state variables. For model (1) also the stiffness coefficient $k(t)$ is a state variable.
- Thanks to the assumption of first-order dynamics of both the damping and stiffness, if the i th damping control variable is limited ($c_{\min} \leq c_{i,\text{in}}(t) \leq c_{\max}$), also the actual coefficient remains in that interval ($c_{\min} \leq c_i(t) \leq c_{\max}$). Similarly, for model (1), the condition $k_{\min} \leq k_{\text{in}}(t) \leq k_{\text{MAX}}$ implies $k_{\min} \leq k(t) \leq k_{\text{MAX}}$. The parameters c_{\min} , c_{\max} , k_{\min} , k_{MAX} represent the limits of the actuators.
- The models adopted for the controllable dampers and springs differ from the ideal behaviour ($c_i(t) = c_{i,\text{in}}(t)$ and $k(t) = k_{\text{in}}(t)$) since first-order linear dynamics are assumed. The ideal behaviour can be approximated by using $\gamma \rightarrow \infty$ and $\beta \rightarrow \infty$ an experimental evaluation is reported in [44]).
- The spring and the damper that constitute a suspension must have the same relative elongation since these devices are linked. This constraint is guaranteed by the algebraic relations $L_{k1} = L_{c1}$ and $L_{k2} = L_{c2}$ (model (2)), and $L_{k1} = L_{\text{cr}}$ (model (3)).

2.1. Remark: stability and robustness of IS, ADS and DSS control systems

The controllable devices in models (2) and (3) are shock absorbers, which have no influence on the equilibrium point. The steady-state derives from the stiffness values of the springs (and their unloaded length) and from the comprised masses. Model (1) may switch between two different springs, so in principle two equilibrium points are possible. However, with an appropriate choice of the unloaded lengths ($\Delta_s = \Delta_{\min}$ for k_{\min} and $\Delta_s = \Delta_{\max}$ for k_{\max}), it is possible to obtain a unique equilibrium point regardless of the stiffness value k_{\min} and k_{\max} .

Due to the presence of only variable damping, models (2) and (3) are strictly passive, hence the equilibrium is stable and robust with respect to any control law of damping and any value of the system parameters [63]. For stability analysis of model (1), assume an ideal (relatively fast) switching of both the springs and the shock absorber. In this situation, the IS model can be regarded as a system commutating among four different stable linear modes. These are characterised by the couples (c_{\min}, k_{\min}) , $(c_{\min}, k_{\text{MAX}})$, $(c_{\text{MAX}}, k_{\min})$ and $(c_{\text{MAX}}, k_{\text{MAX}})$. Each i th mode of the switching system is associated with a state matrix A_i . It is easy to see (by solving the related Linear Matrix Inequality (LMI) [64]) that there exists a positive definite matrix P , so that $A_i'P + A_iP < 0$ for any i . According to the results on stability of switching systems reported in [65] (and references cited therein), model (1) is stable with respect to any possible switching control (global uniform asymptotical stability).

As a first step, for control design purposes, it is interesting to understand if the three systems (1)–(3) are comparable in their controllability range, that is, in correspondence of the boundary values of the coefficients of controllable spring (as for model (1)) and of controllable dampers (as for models (2) and (3)). This basic analysis has been first developed in [34], with reference to the IS and ADS architectures. It is easy to see that:

- If the damping coefficient $c_1(t) \rightarrow \infty$, then the suspension system (2) is reduced to an ideal quarter-car equipped with a classical semi-active suspension composed by spring k_2 and

the variable damper $c_2(t)$. Similarly, if the value of $c_1(t)$ is comparable with $c_2(t)$, the resulting suspension can be considered as an ideal quarter-car equipped with an equivalent spring given by the series of k_1 and k_2 .

- If $c_r(t) \rightarrow 0$, then the suspension system (3) is reduced to a standard semi-active system with the shock absorber $c_s(t)$ and with an equivalent spring resulting from the series of k_1 and k_2 . On the other hand, if $c_r(t) \rightarrow \infty$ the equivalent suspension is made up of the spring k_2 and the controllable damper $c_s(t)$.

Table 1 summarises the passive settings used for comparison of the three configurations; the comparison is done by considering the two extreme settings of the standard (single damper, single spring) configurations: $k = k_{\min}$; $c = c_{\min}$, and $k = k_{\max}$; $c = c_{\max}$. Figure 2 shows the bode magnitude plots of the *comfort* transfer functions (from road profile $z_r(t)$ to the body acceleration $\ddot{z}(t)$) for the systems (1)–(3), (for computation see, e.g. [14,56]). The graphs are related to the two extreme configurations $k = k_{\min}$; $c = c_{\min}$, and $k = k_{\max}$; $c = c_{\max}$, represented in Table 1. Notice that the bode plots are nearly indiscernible. This confirms that the three suspension architectures provide the same results in correspondence to the boundary of controllability range.

It is interesting to observe that one of the possible implementation of DSS and ADS architectures may be based on the use of a standard hydro-pneumatic technology, constituted by: an hydraulic cylinder; two accumulators with different sizes; two electronically controlled electro-valves (EVs). By different positioning of the two EVs, it is possible to implement the two different architectures (Figure 3):

- In the DSS architecture (model (2)), each EV manages the oil flowing in each accumulator.
- The ADS architecture (model (3)) can be implemented by plugging one EV in the common pipe coming from the main cylinder (this valve, named EV-S, implements the damping coefficient $c_s(t)$). The other EV regulates the flux towards one accumulator only.

Table 1. Parameters settings for the dynamical equivalence between the three suspensions systems.

| IS | DSS | ADS |
|------------------------------|-------------------------------|-------------------------------|
| $k = k_{\min}; c = c_{\min}$ | $c_1 = c_2 = c_{\min}$ | $c_r \ll c_s; c_s = c_{\min}$ |
| $k = k_{\max}; c = c_{\max}$ | $c_1 \gg c_2; c_2 = c_{\max}$ | $c_r \gg c_s; c_s = c_{\max}$ |

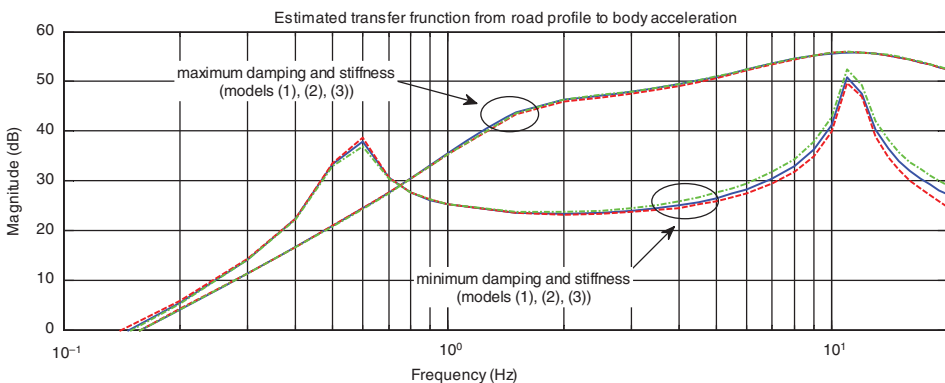


Figure 2. Comparison of the bode magnitude plots in extreme configurations of the three suspension systems (Table 1). Model (1), blue solid line; model (2), green dashed line; model (3), red dotted line.

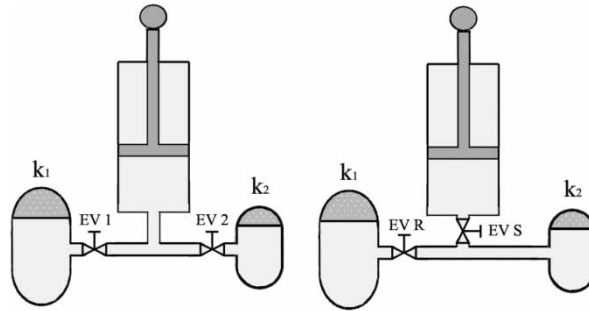


Figure 3. Implementation of a DSS architecture (left) and an ADS architecture (right).

3. Analysis of suspensions with variable damping and stiffness

In this section, the main advantages and trade-offs of a suspension with variable damping and stiffness will be briefly analysed and discussed. In particular, the following two main issues will be considered:

- What is the influence of the (fixed) spring stiffness, in a classical variable-damping semi-active suspension?
- Assuming fast-switching damping and stiffness, what is the best possible performance achievable?

The discussion of the above two issues provides the general framework for the development of variable-damping-and-stiffness semi-active algorithms, which will be presented in the next section.

3.1. Sensitivity to stiffness in a variable-damping semi-active suspension

Today, variable-damping semi-active suspensions seem to be the best compromise between achievable performances, complexity and costs of the system [1,6,21,23,28,45,62,66]. A suspension system provided by a semi-active actuator appropriately controlled is the starting point of this work.

In previous papers [14,42], it was shown the mix-SH-ADD control algorithm provides the best performance, since it almost perfectly meets the filtering limit of a variable-damping semi-active suspension.

The implementation of the mix-SH-ADD control algorithm requires a two-state controllable damper; with reference to the notation in model (1), the control law is given by

$$\begin{cases} c_{in}(t) = c_{max} & \text{if } [(\ddot{z}^2 - \alpha^2 \dot{z}^2) \leq 0 \text{ AND } \dot{z}(\dot{z} - \dot{z}_t) > 0] \text{ OR } [(\ddot{z}^2 - \alpha^2 \dot{z}^2) > 0 \\ & \text{AND } \ddot{z}(\dot{z} - \dot{z}_t) > 0] \\ c_{in}(t) = c_{min} & \text{if } [(\ddot{z}^2 - \alpha^2 \dot{z}^2) \leq 0 \text{ AND } \dot{z}(\dot{z} - \dot{z}_t) \leq 0] \text{ OR } [(\ddot{z}^2 - \alpha^2 \dot{z}^2) > 0 \\ & \text{AND } \ddot{z}(\dot{z} - \dot{z}_t) \leq 0]. \end{cases} \quad (4)$$

This control rationale is extremely simple since it is based on a static rule, which makes use of \dot{z} , \ddot{z} , $(\dot{z} - \dot{z}_t)$ only. This strategy is based on an effective time-domain frequency selector which chooses appropriately either the SH control [29] or the ADD control [42], when the suspension shows either low- or high-frequency behaviours, respectively.

Starting from the classical variable-damping architecture, the mixed SH-ADD has been applied to the suspension model (1) with three different fixed values of stiffness:

$k_{in}(t) = \{k_{min}; k_{nom}; k_{max}\}$. These three variable-damping semi-active configurations have been compared with the 'passive baseline', characterised by fixed damping and stiffness: $k_{in}(t) = k_{nom}, c_{in}(t) = c_{nom}$. The results of this analysis are condensed in Figure 4, where the approximate frequency responses from the road profile to the body acceleration are displayed (see, e.g. [42,43] and references therein, for the description of the method used for their computation). Taking into account that available suspension travel is assumed to be unlimited, from inspecting Figure 5, the following conclusion can be drawn:

- By comparing the 'passive baseline' ($k_{in}(t) = k_{nom}, c_{in}(t) = c_{nom}$), and the variable-damping semi-active suspension with $k_{in}(t) = k_{nom}$, it is clear that the advantage of using a variable-damping semi-active system: the filtering effect of the suspension is uniformly better than its passive counterpart, with no undesired side-effects. For a detailed analysis on optimality and sensitivity of rule (4) with respect to its passive baseline and system parameters, interested readers are referred to [14,42].

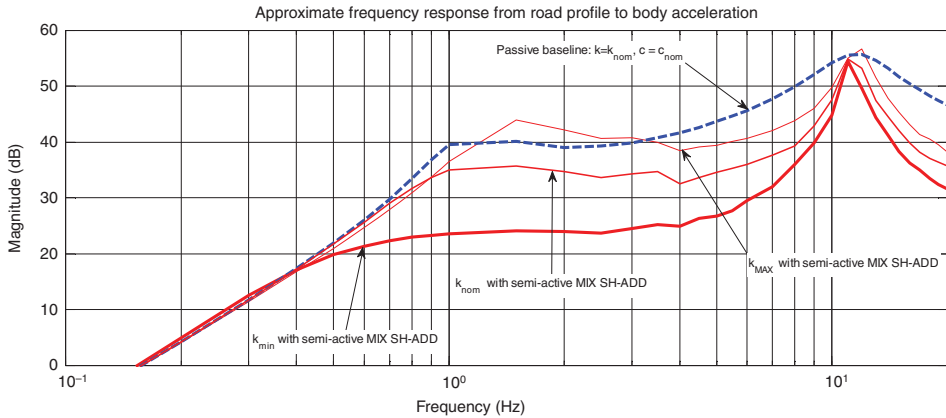


Figure 4. Approximate frequency response of three configurations (corresponding to three values of spring stiffness) of a variable-damping semi-active suspension based on the mixed ADD-SH algorithm. For comparison, a classical 'passive' baseline is shown.

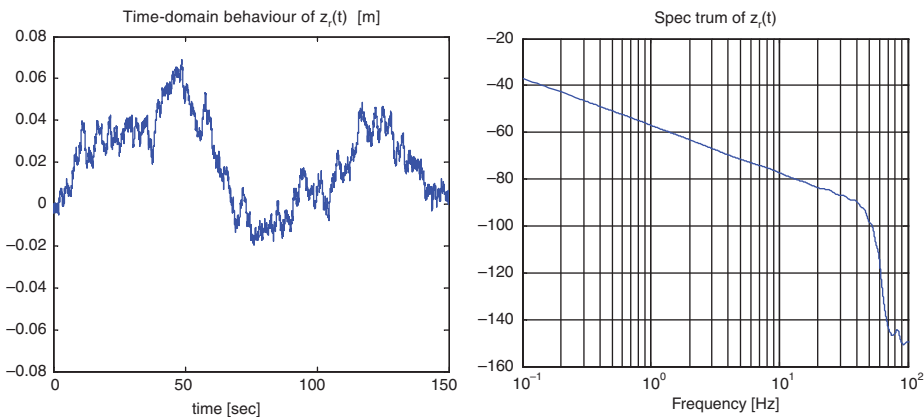


Figure 5. Standard road-profile $\bar{z}_r(t)$ (displayed in the time-domain, over a 150s time window and in the frequency-domain).

- By comparing the three semi-active configurations (with $k_{in}(t) = \{k_{min}; k_{nom}; k_{max}\}$), it is clear that the lower is the suspension stiffness, the better is the filtering effect. Again, by combining a low-stiffness suspension with a good semi-active control strategy, which avoids undesired movements of the vehicle, there are no side-effects in terms of poor damping of the resonances. Moreover, it is worth noticing that the effect of reducing the stiffness in a semi-active suspension is larger than the effect of transforming a standard passive suspension into a variable-damping suspension, with the same spring stiffness.

This simple analysis clearly shows the large potential benefit of changing the stiffness in a classical variable-damping semi-active suspension. However, this analysis hides the fact that the main side-effect of lowering the spring stiffness is that the actual suspension travel grows; the available stroke of a suspension hence may become the real limit for a semi-active suspension with an appropriate damping control.

In order to analyse how the introduction of the stroke limits affects the overall performances, it is necessary to embed a modified model of the spring stiffness, and to define a simulation test for the performance evaluation. An effective way of modelling the stroke limits (end-stops) of a suspension is to redefine the equations on the suspension spring $k(t)$ as follows (with reference to Equation (1)):

$$\begin{aligned} \dot{k}(t) &= -\beta'k(t) + \beta'k_{in}(t) \quad \text{if } |z - z_t - \Delta_s| < \Lambda \\ k(t) &= K \quad \text{if } |z - z_t - \Delta_s| \geq \Lambda; K \gg k_{max} \\ k_{in}(t) &\in [k_{min}, k_{max}]. \end{aligned} \quad (5)$$

Symbols in Equation (5) have the same meaning as the symbols of model (1). Λ is the available stroke; K represents an ‘equivalent stiffness’ of the end-stop zone; it is much higher than k_{max} (it is the typical stiffness of rubber bushings).

In order to highlight the trade-off arising from the introduction of the end-stops, the following evaluation test is defined:

- A standard road profil $\bar{z}_r(t)$ is designed as an integrated white noise (random walk), band-limited within the frequency range 0–30 Hz (Figure 5). Its maximum amplitude is $\bar{A} = 0.07$ m. Notice that this kind of signal is able to excite all the frequency of interest and resembles a realistic mild off-road profile [40].
- During the test, the damping is controlled using the mixed SH–ADD algorithm. Again, the variable-damping semi-active suspension system is compared with the range (k_{min}, k_{max}) . The simulation test is repeated with and without end-stops ($\Lambda = 0.2$ m is used, which represents the typical available stroke for a suspension of a vehicle designed for mild off-road conditions).

The effect of the introduction of the end-stops is displayed in Figure 6, where the body accelerations $\ddot{z}(t)$ and the suspension travel $z(t) - z_t(t)$ are plotted. Clearly, reaching the end-stop causes a dramatic deterioration of the comfort performances.

The effect of reaching the end-stops may be also observed in the frequency-domain represented in Figure 7. This figure shows the approximate transfer function from the road profile $z_r(t)$ to the body acceleration $\ddot{z}(t)$ of the suspension simulated with and without end-stops (for the computation of the approximate transfer function of a suspension system fed by a broadband signal see, e.g. [14,43]). Notice that the impulsive acceleration peaks caused by the limited stroke travel and revealed in Figure 6 seem to affect the approximate transfer function only beyond the wheel resonance (15 Hz). This representation may be misleading since the suspension performances seem to be comparable with the bandwidth of the main

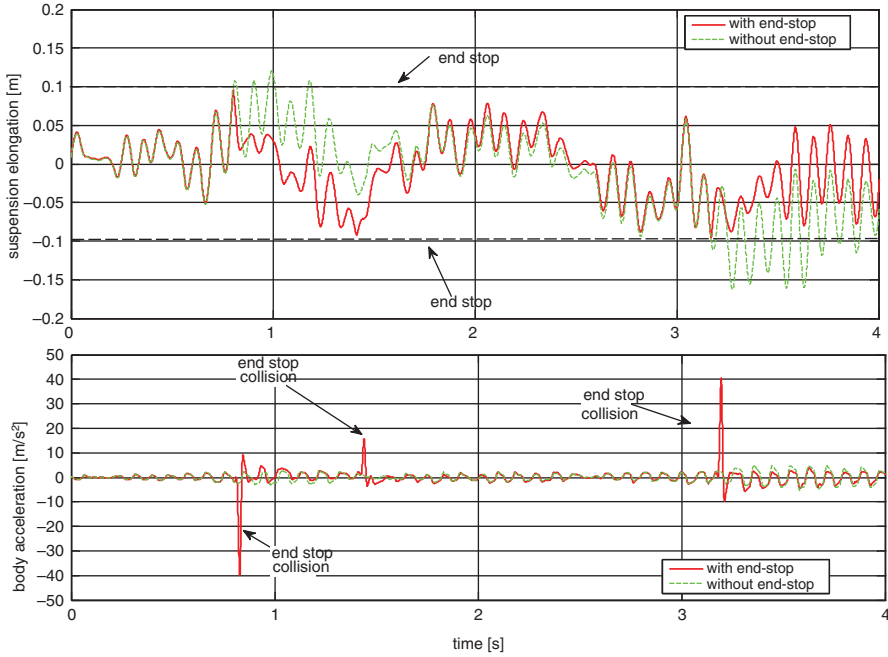


Figure 6. Time history of the suspension stroke (top) and the body acceleration (bottom), with and without the end-stops.

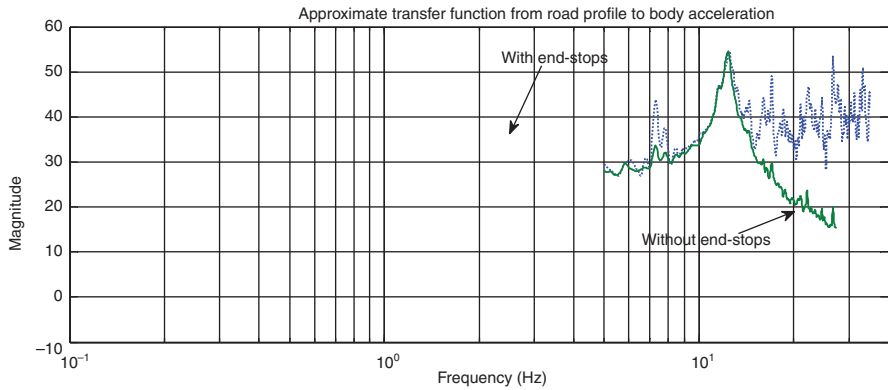


Figure 7. Approximate transfer function from the road profile to the body acceleration with and without end-stops.

system dynamics (0–15 Hz). Further, the acceleration peaks are so numerically represented as a broadband noise beyond 15 Hz.

In order to better assess the suspension performances, the following indices can be taken into account:

$$J = \sqrt{\frac{\int_0^T (\ddot{z}(t))^2 dt}{\int_0^T (\ddot{z}_r(t))^2 dt}} \tag{6}$$

$$J_{el} = \max |z - z_t|. \tag{7}$$

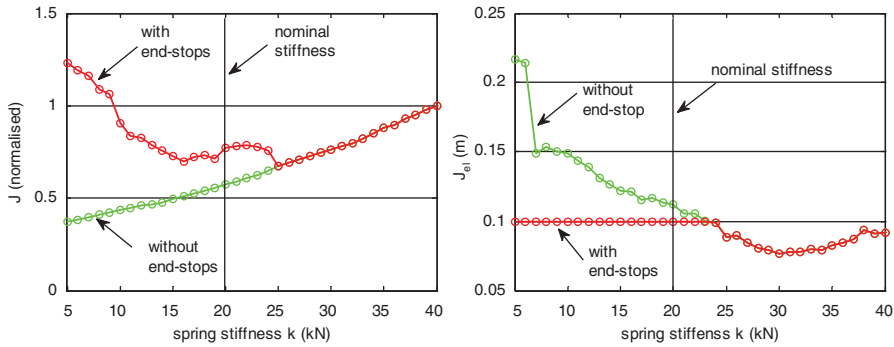


Figure 8. Disturbance transmission (left) and maximum suspension elongation (right) for suspensions with controlled damping, with respect to the spring stiffness ($k \in [k_{\min}, k_{\max}]$). Without end-stops (green line); with end-stops (red line).

Both indices are computed assuming the standard road profile $\bar{z}_r(t)$ as input. Note that Equation (6) is the L_2 norm of $\ddot{z}(t)$ normalised with respect to the L_2 norm of the road disturbance $\bar{z}_r(t)$; it is commonly used as the comfort index for evaluating the suspension system performances [1,5,19,51], and it represents a concise measure of the overall body motion. The index (7) is very simple and provides a measure of the required stroke travel for a particular working condition.

Considering a suspension with controllable damping and limited stroke travel, it is interesting to understand the potential compromises related to the design of spring stiffness. Notice that with damping control available, the choice of the spring coefficient can be driven by considerations that differs from those for the classical suspension design. For this purpose, the IS model (with damping controlled by rule (4)) has been fed by $\bar{z}_r(t)$, and simulated with several levels of stiffness ($k \in [k_{\min}; k_{\max}]$ with a 1000 N/m step). The results are summarised in Figure 8, where the performance indices (6) and (7) are displayed. The analysis of Figure 8 clearly shows that:

- The dependence of the results with respect to the spring coefficient k is extremely nonlinear; this is mainly due to the control of damping which introduces a strong nonlinearity into the system dynamics.
- The best performances in terms of comfort are guaranteed by a suspension with unlimited stroke travel. In this situation, a very low level of spring stiffness shows the best disturbance filtering (the softer the better). Notice that this is ensured by the optimal control of damping achieved by the SH-ADD rule.
- When the end-stops are included, a compromise arises in the suspension system. In terms of body dynamics, the best spring stiffness is the softer spring that is simultaneously able to avoid the end-stop (in Figure 8 this is $k = 25$ KN/m). Notice that, however, the disturbance transmission is far to be as optimal as the one achieved with a soft spring and unlimited stroke travel. It would be interesting to understand if an appropriate control of stiffness may manage the stroke travel in a better way and provide good comfort without hard stops.

3.2. Optimal predictive control: the benchmark

Before developing algorithms to control both variable damping and stiffness (see next section), it is useful to understand the lower bound of the filtering capability of such a semi-active suspension system. This analysis is worked out in an ‘ideal’ setting: the IS model (1) is considered, perfect knowledge (also in the future) of the road disturbance is assumed, and no

limits on the computational complexity are given. This analysis is very useful since it clearly sets a benchmark: every 'real' algorithm must be compared with such a lower bound [14] where a similar analysis is discussed for classical variable-damping semi-active suspensions).

Consider an ideal semi-active suspension with variable damping and stiffness and limited stroke travel, as described by Equations (1) and (5). Consider that the parameters of the controllable shock absorber and spring (c_{\min} , c_{\max} , k_{\min} , k_{\max} , β , and γ) are fixed. Moreover, assume that $c_{\text{in}}(t) = \{c_{\min}, c_{\max}\}$ and $k_{\text{in}}(t) = \{k_{\min}, k_{\max}\}$ (two-state dampers and two-state springs), so that the control action must select, at every sampling time, one out of four possible damping–stiffness combinations:

$$(c_{\text{in}}(t), k_{\text{in}}(t)) = \{(c_{\min}, k_{\min}); (c_{\min}, k_{\max}); (c_{\max}, k_{\min}); (c_{\max}, k_{\max})\}.$$

As theoretically proven in [42], this is a non-restrictive assumption for controllable suspension, provided that the actuation bandwidth is sufficiently large, and the sampling time ΔT of the digital controller is sufficiently small.

The design problem of the control algorithm can be reduced to the following: consider a time window $[0, T]$, fixed initial conditions, and a given road profile $\tilde{z}_r(t)$ and $t \in [0, T]$; consider the global performance index

$$J^* = \frac{\int_0^T (\ddot{z}(t))^2 dt}{\int_0^T (\ddot{z}_r(t))^2 dt} \quad (8)$$

find the sequence of digital control inputs ($c_{\text{in}}(1 \cdot \Delta T)k_{\text{in}}(1 \cdot \Delta T)$), ($c_{\text{in}}(2 \cdot \Delta T)k_{\text{in}}(2 \cdot \Delta T)$) \cdots ($c_{\text{in}}(k \cdot \Delta T)k_{\text{in}}(k \cdot \Delta T)$) \cdots ($c_{\text{in}}(H \cdot \Delta T)k_{\text{in}}(H \cdot \Delta T)$), $H = T/\Delta T$, which minimises J^* . The solution of the above control problem provides the best possible control strategy for the suspension, for that road profile.

In practice, it is impossible to implement in real-time such a globally optimal control strategy on a real system; the main reason is that, in practice, the road profile is unknown. Moreover, even if an *a priori* knowledge of $\tilde{z}_r(t)$, $t \in [0, T]$ is assumed, the optimisation task is formidable: the optimal solution must be searched among 4^H possible sequences of digital control inputs (if $T = 10$ s and $\Delta T = 10$ ms), this means that $H = 1000$, which makes the optimisation task almost impossible to be dealt with). Even if this problem cannot be solved in a real-time implementation, it can be solved numerically offline, if we make some simplifying assumptions (hence considering a *quasi*-optimal predictive control solution).

To this purpose, consider as input the integrated band-limited white noise introduced in the previous section (Figure 6) appropriately scaled by a factor α , so that $\tilde{z}_r(t) = \alpha \tilde{z}_r(t)$. Moreover, use the mixed SH–ADD as the damping-control strategy (proven to be almost optimal and computationally very low demanding). The only 'free choice' hence is the spring stiffness. The stiffness control signal is refreshed with a frequency of 100 Hz ($\Delta T = 10$ ms), and $Q = 10$ switches are taken into consideration, so that we have a prediction window of $\Delta T \cdot Q = 100$ ms and $T/(\Delta T \cdot Q)$ windows. It can be shown that $Q = 10$ is a good compromise between optimality and computational time (see Figure 9 and [14]). In every time window, the optimal solution must be searched among $2^{10} = 1024$ possible sequences. The optimisation task hence is tough but tractable, and the performance index J^* of the *quasi*-optimal predictive control strategy can be computed offline for increasing values of the scaling factor α of the input signal (if $\alpha = 1$, the maximum amplitude of the road disturbance is 7 cm). The results of this numerical analysis are condensed in Figure 10. They are compared with mixed SH–ADD on a traditional variable-damping semi-active architecture.

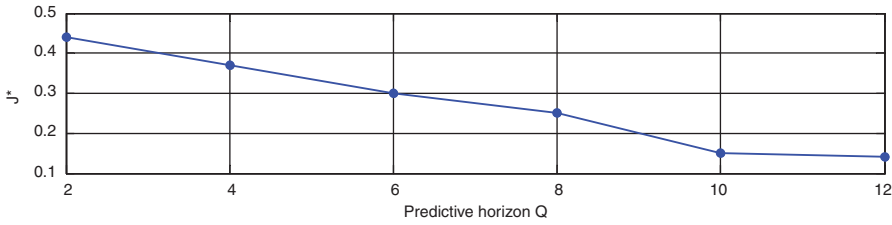


Figure 9. Performances of the quasi-optimal predictive control strategy, with respect to the predictive horizon Q .

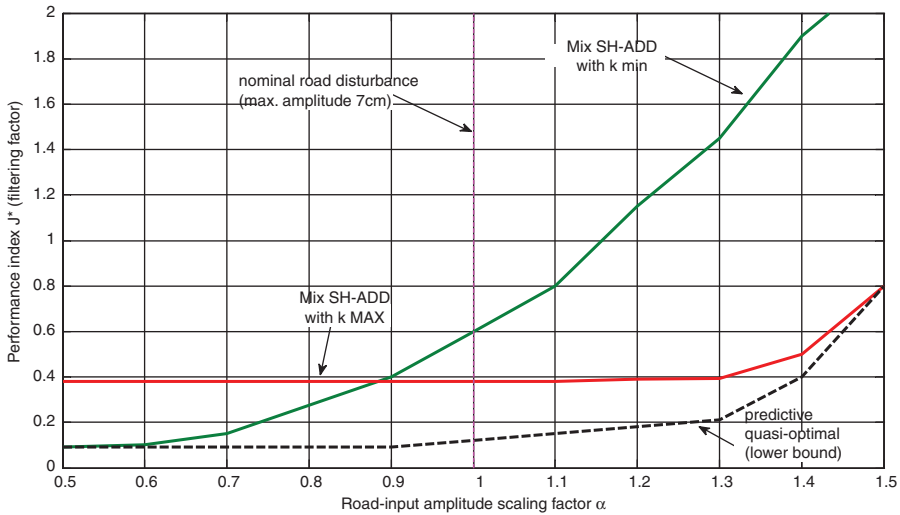


Figure 10. Comparison of the filtering performances of mixed SH-ADD with low spring stiffness, high spring stiffness and the numerically-computed quasi-optimal lower bound, as a function of the road input scaling factor α .

The results condensed in Figure 10 are very interesting, and can be easily interpreted:

- When the road disturbance amplitude is very small (hence it is unlikely to hit the end-stop) the best performances are achieved with a suspension equipped with a soft spring (k_{\min}) and with a controllable damper ruled by the mixed SH-ADD algorithm.
- When the road disturbance amplitude is very large, the suspension equipped with a hard spring (k_{\max}) and with a damper controlled by mixed SH-ADD provides the best performances in terms of overall comfort.
- For the medium amplitude of road displacement, an appropriate stiffness control (it quasi-optimal predictive control) is able to overcome this trade-off and to ensure the best comfort. The optimal filtering capability cannot be achieved by any traditional variable-damping suspension system with fixed spring stiffness.

Considering the above results, it is clear that a variable-damping-and-stiffness electronic suspension has the chance to outperform significantly a traditional variable-damping semi-active suspension. Hence, the next key problem is the following: considering one of the two ‘real’ architectures (DSS and ADS), is it possible to design a simple real-time control algorithm, which achieves the ‘best’ behaviour? This problem will be considered in the following section.

4. Control strategies: the SSTSC algorithm

To overcome the trade-off previously presented, and to approximate the intrinsic filtering limit of the suspension, this paper proposes a simple and innovative control algorithm named *SSTSC*.

This algorithm consists of a dynamic regulation of the suspension stiffness coefficient based on two thresholds (the first acts on the elongation $|z - z_t|$, the second on the elongation-speed $|\dot{z} - \dot{z}_t|$ of the suspension), and on a sign-comparison of elongation and elongation-speed (two-dimensional control). With reference to the symbols used in the IS (model (1)), the control law is the following:

$$\begin{cases} (k_{in}(t) = k_{min}) \text{ AND } (c_{in}(t) = \text{Mixed SH-ADD}) & \text{if } (|z - z_t| \leq t_e) \text{ AND } ((|\dot{z} - \dot{z}_t| \leq t_{es}) \\ & \text{OR } ((z - z_t) \cdot (\dot{z} - \dot{z}_t \leq 0)) \\ (k_{in}(t) = k_{max}) \text{ AND } (c_{in}(t) = \text{Mixed SH-ADD}) & \text{otherwise} \end{cases} \quad (9)$$

where t_e and t_{es} are the thresholds on the elongation and elongation-speed, respectively; these two parameters are the two tuning knobs. Roughly speaking, when the suspension approaches the end-stop or when elongation and elongation-speed have the same sign and elongation-speed exceeds a specified threshold, the algorithm selects a high-virtual stiffness coefficient in order to reduce elongation and to avoid suspension hard stops. In the other cases, the algorithm selects a softer virtual stiffness coefficient, in order to maximise the performance. At the same time, the damping of the suspension is regulated according to the mixed SH-ADD rationale.

In order to tune the parameters t_e and t_{es} , an optimisation procedure has been carried out. To this purpose, the closed-loop system is fed by the integrated band-limited white noise $\bar{z}_r(t)$ (Figure 6) scaled for different values of $\alpha \in [0.5, 1.5]$, and an ‘overall’ cost function is defined as follows:

$$\bar{J}^* = \int_{0.5}^{1.5} J^*(\alpha) d\alpha \quad (10)$$

where

$$J^*(\alpha) = \int_0^T \frac{(\ddot{z}(t))^2 dt}{\int_0^T (\bar{z}_r(t))^2 dt} = \int_0^T \frac{(\ddot{z}(t))^2 dt}{\alpha^2 \int_0^T (\bar{z}_r(t))^2 dt},$$

$J^*(\alpha)$ represents the comfort performance index of the suspension with respect to the specific input amplitude scaled by factor α . \bar{J}^* represents an averaged performance index, over a wide interval of input amplitudes. Parameters t_e , t_{es} thus, can be computed by numerically solving the following optimisation problems:

$$(\hat{t}_e, \hat{t}_{el}) = \operatorname{argmin}_{(t_e, t_{el})} (\bar{J}^*). \quad (11)$$

The SSTSC strategy is designed with reference to the IS (model (1), with conditions (5)); however, it can be implemented in both the suspension architectures (2) and (3) (DSS and ADS), according to the framework presented in Figure 11: the actual system is defined by Equation (2) or (3), complemented with end-stop conditions (5); the control structure monitors measurable states of the system (the body acceleration $\ddot{z}(t)$ and its integrated signals; the suspension elongation $z(t) - z_t(t)$ and its derivative); according to Equation (9), the algorithm selects the damping and stiffness coefficients $c_{in}(t)$ and $k_{in}(t)$, which are mapped into the equivalent damping of DSS or ADS.

To assess the performances of the SSTSC applied to the DSS and ADS architectures, the simulation activity (again, using the random signal of Figure 6, with the scaling factor α) has

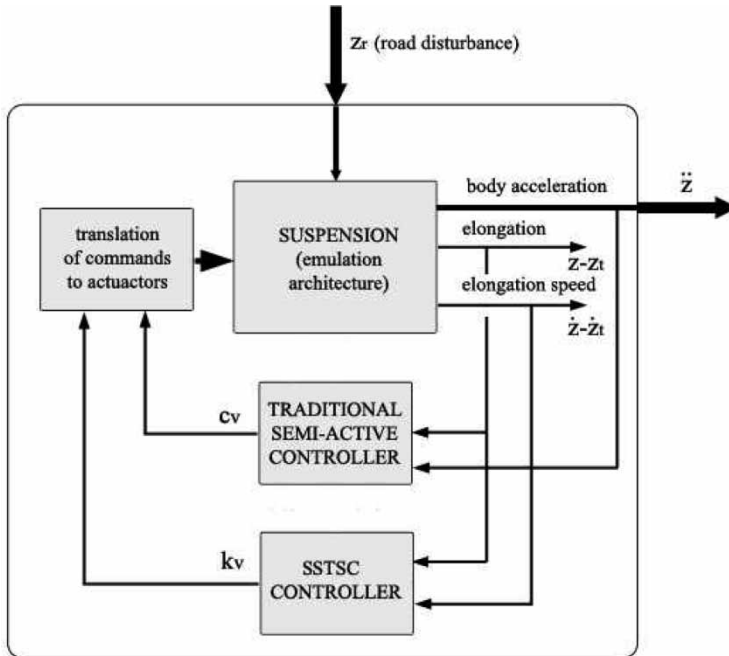


Figure 11. Implementation scheme of the SSTSC algorithm.

been repeated in different configurations:

- SSTSC coupled with mixed SH-ADD, implemented by the DSS architecture;
- SSTSC coupled with mixed SH-ADD, implemented by the ADS architecture;
- Mixed SH-ADD on traditional variable-damping semi-active architecture (evaluated for k_{\min} and k_{\max}).

The results are displayed in Figure 12, where the index J^* is displayed, as a function of the input scaling factor α . The following remarks can be done:

- The optimally tuned DSS and ADS implementations of the SSTSC algorithm provide a similar performance. For a small road-input amplitude, the DSS architecture slightly outperforms ADS; on the contrary, for intermediate values of the input amplitude, ADS is slightly better.
- The SSTSC algorithm significantly outperforms the fixed-stiffness variable-damping semi-active suspension systems: this clearly shows the potential benefit of a variable-damping-and-stiffness suspension system.
- The SSTC algorithm does not reach the lower bound, computed with the quasi-optimal predictive control strategy; however, the loss of performance with respect to the 'ideal' strategy is comparatively small.

The performance of the SSTSC in the DSS and ADS architectures displayed in Figure 12 are referred to an optimal tuning of their design parameters t_e and t_{es} , obtained by solving Equation (11). However, it is important to analyse the sensitivity of the algorithms with respect to different parameter tunings. To this purpose, the performance of the DSS and ADS architectures are displayed in Figure 13, with thresholds in the ranges $t_e \in [0, 0.1]$ and $t_{el} \in [0, 1]$. For each architecture, the entire range of performance (from the best to the worst parameter setting) is displayed. From Figure 13, it is easy to see that the DSS architecture shows a much

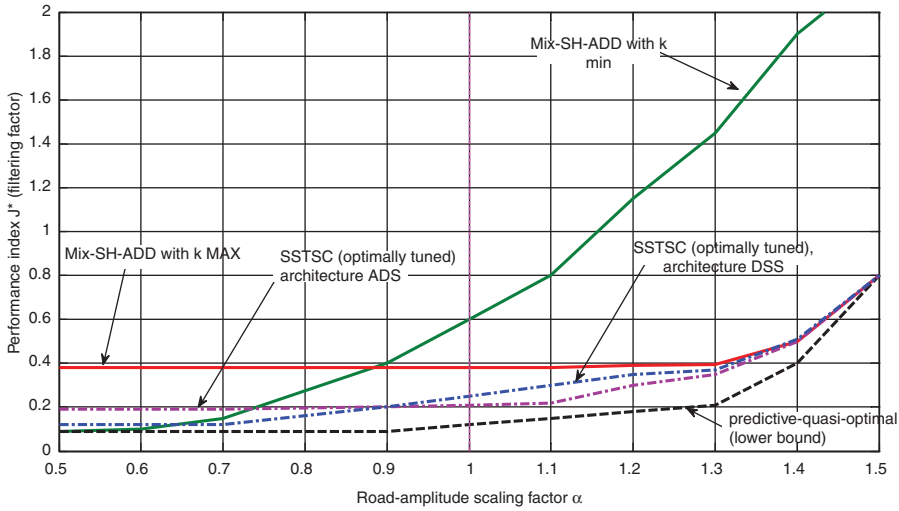


Figure 12. Analysis of the performance of different suspension configurations and algorithms, as a function of the input scaling factor α .

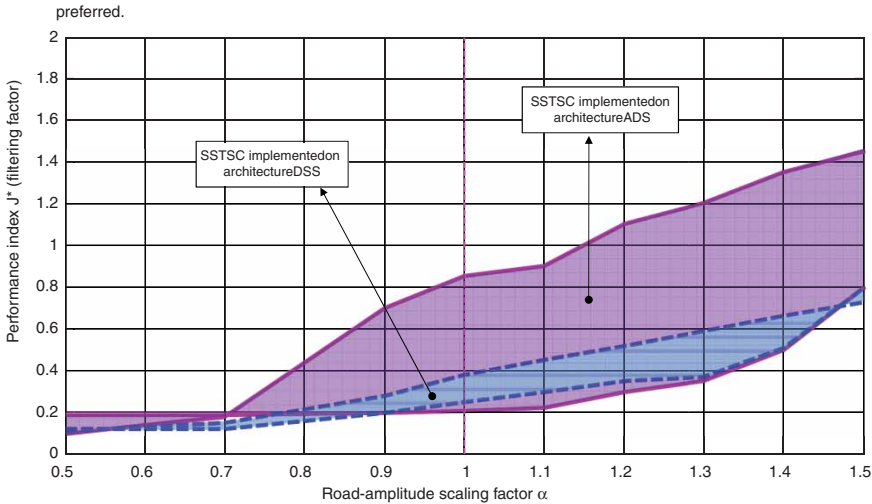


Figure 13. Sensitivity to the algorithm parameters of the SSTSC algorithm, in the DSS and ADS implementations.

lower sensitivity to parameter tuning, especially for medium and large values of the road input amplitude. Due to this very important additional feature, the DSS suspension architecture must be preferred.

To conclude the section, Figure 14 shows a condensed summary of the performance (filtering effect) of different suspension configurations, simulated with the nominal random road input $\bar{z}_r(t)$ (Figure 6), as a function of its amplitude scaling factor α . Five different configurations are compared:

- Two traditional ‘passive’ suspensions, characterised by the extreme settings (k_{\min}, c_{\min}) , (k_{\max}, c_{\max}) .
- Two standard variable-damping suspensions, equipped with the mix-SH-ADD algorithm, at two different fixed values of spring stiffness $(k_{\min}$ and $k_{\max})$.

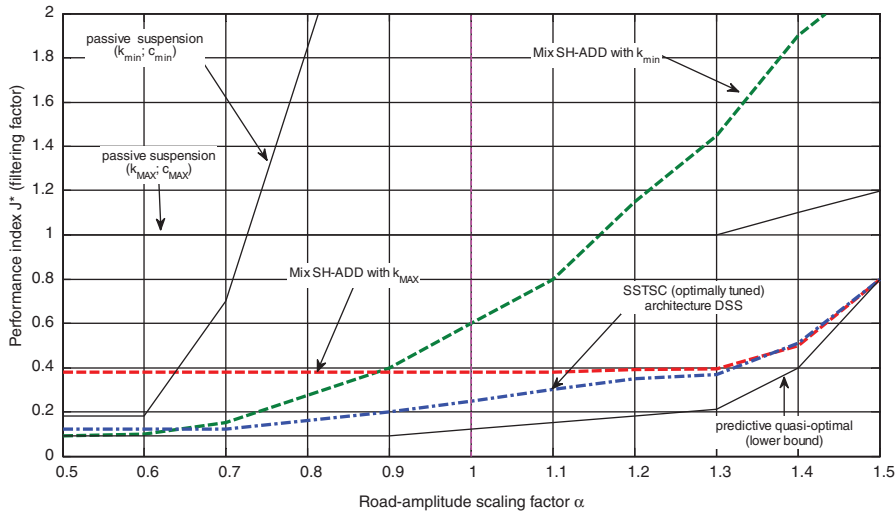


Figure 14. Final comparison of different suspension configurations, as a function of the input scaling factor α . Continuous lines: passive suspensions; dashed lines: variable-damping suspensions; dashed-dotted line: variable-damping-and-stiffness suspension.

- The best variable-damping-and-stiffness suspension; as discussed above, the DSS architecture is preferable, thanks to its lower sensitivity to parameter tuning; the DSS suspension architecture is equipped with the SSTSC algorithm (9).
- The quasi-optimal predictive lower bound is also displayed, to provide a lower bound of the best possible performance achievable.

By inspecting Figure 14, the following conclusions can be drawn:

- By focusing on the three traditional passive configurations, notice that the spread of performance is very large, and very dependent on the road-input amplitude. This clearly shows that, in a traditional suspension, the problem of finding the correct trade-off to tune the fixed values of damping and stiffness is a formidable task.
- By inspecting the two variable-damping semi-active suspensions, it is apparent that, thanks to the variable-damping capability (if coupled with a wise algorithm), the spread of performance is significantly reduced, when compared with the passive suspension. The benefit is a higher robustness of performance in different road conditions. However, the choice of the fixed value of stiffness is still a non-trivial issue, which has no unique solution.
- The variable-damping-and-stiffness semi-active suspension highly improves the robustness of the suspension system, with respect to different road input conditions. Notice that the filtering capability of the SSTSC–DSS suspension significantly (and uniformly) outperforms any other suspension configuration (even if it is still not capable of fully exploiting the theoretical capability of a variable-damping-and-stiffness suspension).

5. Conclusive remarks and future work

Starting from a suspension with controllable dampers, this paper has studied how in a semi-active framework, a control of the stiffness may improve the suspension performances. For this purpose, two different suspension architectures (DSS and ADS), capable of implementing ‘in practice’ a variable-damping-and-stiffness suspension, have been proposed and discussed.

An analysis of the potential benefits and trade-offs provided by using a variable-stiffness suspension system is proposed. Then, using an optimal predictive control framework, the lower bound of the performances achievable with a variable-damping-and-stiffness suspension system has been numerically computed. An algorithm (named SSTSC) for the joint control of damping and stiffness is proposed and analysed.

This work has shown the remarkable potential benefits of a variable-damping-and-stiffness suspension architecture, obtained with practically implementable suspension systems, and a simple but effective control algorithm. This work represents one of the very first attempts to study genuine variable-damping-and-stiffness semi-active suspensions systems. The research on this topic is now being developed along two mainstreams: the set-up of a real suspension system, for the experimental validation of the theoretical and simulation-based results obtained in this work, and the further development of the control algorithm.

References

- [1] R. Isermann, *Mechatronic Systems: Fundamentals*, Springer Verlag, UK, 2003.
- [2] M. Bieber, S.M. Mackool, and D.S. Rhode, *Vehicle suspension control systems*, Patent US 5,864,768, 1999.
- [3] M.C. Campi, A. Lecchini, and S.M. Savaresi, *An application of the virtual reference feedback tuning (VRFT) method to a benchmark active suspension system*, Eur. J. Control 9 (2003), pp. 66–76.
- [4] I. Fialho and G.J. Balas, *Road adaptive active suspension design using linear parameter-varying gain-scheduling*, IEEE Trans. Control Syst. Tech. 10 (2002), pp. 43–54.
- [5] D. Fischer and R. Isermann, *Mechatronic semi-active and active vehicle suspensions*, Control Eng. Pract. 12(11) (2003), pp. 1353–1367.
- [6] E. Foo and R.M. Goodall, *Active suspension control of flexible-bodied railway vehicles using electro-hydraulic and electro-magnetic actuators*, Control Eng. Pract. 8 (2000), pp. 507–518.
- [7] W. Fu-Cheng and M.C. Smith, *Controller parameterization for disturbance response decoupling: Application to vehicle active suspension control*, IEEE Trans. Control Syst. Tech. 10(3) (2002), pp. 393–407.
- [8] K. Fujimori, K. Hayakawa, H. Kimura, K. Matsumoto, Y. Suzuki, and M. Yamashita, *Robust H_∞ output feedback control of decoupled automobile active suspension systems*, IEEE Trans. Autom. Control 44(2) (1999), pp. 392–396.
- [9] T.D. Gillespie, *Fundamentals of Vehicle Dynamics*, Society of Automotive Engineers Inc, Warrendale, PA, 1992.
- [10] G.O. Guardabassi and S.M. Savaresi, *Approximate linearization via feedback – an overview*, Automatica (survey paper) 37(1) (2001), pp. 1–15.
- [11] D. Hrovat, *Survey of advanced suspension developments and related optimal control applications*, Automatica 33(10) (1997), pp. 1781–1817.
- [12] U. Kiencke and L. Nielsen, *Automotive Control Systems for Engine, Driveline, and Vehicle*, Springer Verlag, New York, 2000.
- [13] D.H. Reed and S.T. Radcliffe, *Output filter and method for on/off semi-active suspension system*, US Patent 5,024,460, 1991.
- [14] S.M. Savaresi and C. Spelta, *Mixed sky-hook and ADD: Approaching the filtering limits of a semi-active suspension*, ASME Trans. J. Dyn. Syst. Meas. Control 129(4) (2007), pp. 382–392.
- [15] S.M. Savaresi, M. Tanelli, and C. Cantoni, *Mixed slip-deceleration control in automotive braking systems*, ASME Trans. J. Dyn. Syst. Meas. Control 129(1) (2007), pp. 20–31.
- [16] M.W. Sayers, *Vehicle models for RTS applications*, Veh. Syst. Dyn. 32 (1999), pp. 421–438.
- [17] E. Silani, S.M. Savaresi, S. Bittanti, D. Fischer, and R. Isermann, *Managing information redundancy for the design of fault-tolerant slow-active controlled suspension*, Tire Technol. Int. 2004 (2004), pp. 128–133.
- [18] M. Valasek, W. Kortum, Z. Sika, L. Magdolen, and O. Vaculin, *Development of semi-active road-friendly truck suspensions*, Control Eng. Pract. 6 (1998), pp. 735–744.
- [19] R.A. Williams, *Automotive active suspensions part 1: Basic principles*, Proc. Inst. Mech. Eng. D 211 (1997), pp. 415–426.
- [20] K. Yoshida and B. Okamoto, *Bilinear disturbance-accommodating optimal control of semi-active suspension for automobiles*, IEEE International Conference on Control Applications, 1999, pp. 1496–1501.
- [21] M. Ahmadian, B.A. Reichert, and X. Song, *System nonlinearities induced by skyhook dampers*, Shock Vib. 8(2) (2001), pp. 95–104.
- [22] R. Caponetto, O. Diamante, G. Fargione, A. Risitano, and D. Tringali, *A soft computing approach to fuzzy sky-hook control of semi-active suspension*, IEEE Trans. Control Syst. Tech. 11(6) (2003), pp. 786–798.
- [23] S.B. Choi, J.H. Choi, Y.S. Lee, and M.S. Han, *Vibration control of an ER seat suspension for a commercial vehicle*, ASME J. Dyn. Syst. Meas. Control 125(1) (2003), pp. 60–68.
- [24] S.B. Choi, D.W. Park, and M.S. Suh, *Fuzzy sky-ground hook control of a tracked vehicle featuring semi-active electrorheological suspension units*, ASME J. Dyn. Syst. Meas. Control 124(1) (2002), pp. 150–157.

- [25] A. General Gelb and W.E. Van der Velde, *Multiple-Input Describing Functions and Nonlinear System Design*, McGraw-Hill, New York, 1968.
- [26] A. Giua, C. Seatzu, and G. Usai, *Semiactive suspension design with an optimal gain switching target*, Veh. Syst. Dyn. 31(4) (1999), pp. 213–232.
- [27] R.M. Goodall and W. Kortüm, *Mechatronic developments for railway vehicles of the future*, Control Eng. Pract. 10 (2002), pp. 887–898.
- [28] K.S. Hong, H.C. Sohn, and J.K. Hedrick, *Modified skyhook control of semi-active suspensions: A new model, gain scheduling, and hardware-in-the-loop tuning*, ASME J. Dyn. Syst. Meas. Control 124(1) (2003), pp. 158–167.
- [29] D.C. Karnopp and M.J. Cosby, *System for controlling the transmission of energy between spaced members*, US Patent 3,807,678, 1974.
- [30] T. Kawabe, O. Isobe, Y. Watanabe, S. Hanba, and Y. Miyasato, *New semi-active suspension controller design using quasi-linearization and frequency shaping*, Control Eng. Pract. 6(10) (1998), pp. 1183–1191.
- [31] K.J. Kitching, D.J. Cole, and D. Cebon, *Performance of a semi-active damper for heavy vehicles*, ASME J. Dyn. Syst. Meas. Control 122(3) (2000), pp. 498–506.
- [32] H. Li and R.M. Goodall, *Linear and non-linear skyhook damping control laws for active railway suspensions*, Control Eng. Pract. 7 (1999), pp. 843–850.
- [33] W.H. Liao and D.H. Wang, *Semiactive vibration control of train suspension systems via magnetorheological dampers*, J. Intell. Mater. Syst. Struct. 14(3) (2003), pp. 161–172.
- [34] Y. Liu, H. Matsuhsiaa, and H. Utsunoa, *Semi-active vibration isolation system with variable stiffness and damping control*, J. Sound Vib. 313(1–2) (2008), pp. 16–28.
- [35] A.J. Nieto, A.L. Moralesa, A. González, J.M. Chicharro, and P. Pintadoa, *An analytical model of pneumatic suspensions based on an experimental characterization*, J. Sound Vib. 313(1–2) (2008), pp. 290–307.
- [36] H. Nakai, S. Oosaku, and Y. Motozono, *Application of practical observer to semi-active suspensions*, ASME J. Dyn. Syst. Meas. Control 122(2) (2000), pp. 284–289.
- [37] E. Papadopoulos and I. Papadimitriou, *Modeling, design and control of a portable washing machine during the spinning cycle*, Proceedings of the 2001 IEEE/ASME International Conference on Advanced Intelligent Mechatronics Systems, 2001.
- [38] R. Pintelon and J. Schoukens, *System Identification: A Frequency Domain Approach*, IEEE Press, New York, 2001.
- [39] I. Pratt and R. Goodall, *Controlling the ride quality of the central portion of a high-speed railway vehicle*, American Control Conference, Vol. 1, 1997, pp. 719–723.
- [40] J.D. Robson and C.J. Dodds, *The response of vehicle component to random road-surface undulations*, 13th FISITA Congress, Brussels, Belgium, 1970.
- [41] S.M. Savaresi, S. Bittanti, and M. Montiglio, *Identification of semi-physical and black-box non-linear models: The case of MR-dampers for vehicles control*, Automatica 41 (2005), pp. 113–117.
- [42] S.M. Savaresi, E. Silani, and S. Bittanti, *Acceleration-driven-damper (ADD): An optimal control algorithm for comfort-oriented semi-active suspensions*, ASME Trans. J. Dyn. Syst. Meas. Control 127(2) (2005), pp. 218–229.
- [43] S.M. Savaresi, E. Silani, S. Bittanti, and N. Porciani, *On performance evaluation methods and control strategies for semi-active suspension systems*, 42nd Control and Decision Conference, Maui, HI, 2003, pp. 2264–2269.
- [44] S.M. Savaresi and C. Spelta, *A single-sensor control strategy for semi-active suspensions*, IEEE Trans. Control Syst. Tech. 17(1) (2009), pp. 143–152.
- [45] S.M. Savaresi and C. Spelta, *Method and apparatus for controlling a semi-active suspension*, International Patent WO/2008/010075, 2006.
- [46] S.M. Savaresi, M. Tanelli, P. Langthaler, and L. Del Re, *New regressors for the direct identification of tire-deformation in road vehicles via ‘in-tire’ accelerometers*, IEEE Trans. Control Syst. Tech. 16(4) (2008), pp. 769–780.
- [47] S.M. Savaresi, F. Taroni, F. Previdi, and S. Bittanti, *Control system design on a power-split CVT for high-power agricultural tractors*, IEEE/ASME Trans. Mechatronics 9(3) (2004), pp. 569–579.
- [48] E. Silani, S.M. Savaresi, S. Bittanti, A. Visconti, and F. Farachi, *The concept of performance-oriented yaw-control systems: Vehicle model and analysis*, SAE Trans. J. Passenger Cars Mech. Syst. 2002 (2003), pp. 1808–1818.
- [49] A. Stribersky, H. Müller, and B. Rath, *The development of an integrated suspension control technology for passenger trains*, Proc. Inst. Mech. Eng. F 212 (1998), pp. 33–42.
- [50] H.E. Tseng and J.K. Hedrick, *Semi-active control laws – optimal and sub-optimal*, Veh. Syst. Dyn. 23 (1994), pp. 545–569.
- [51] R.A. Williams, *Automotive active suspensions part 2: Practical considerations*, Proc. Inst. Mech. Eng. D 211 (1997), pp. 427–444.
- [52] V.S. Atray and P.N. Roschke, *Design, fabrication, testing, and fuzzy modeling of a large magnetorheological damper for vibration control in a railcar*, IEEE/ASME Joint Rail Conference, 2003, pp. 223–229.
- [53] S.M. Savaresi, R. Bitmead, and W. Dunstan, *Nonlinear system identification using closed-loop data with no external excitation: The case of a lean combustion process*, Int. J. Control 74 (2001), pp. 1796–1806.
- [54] B.F. Spencer Jr, S.J. Dyke, M.K. Sain, and J.D. Carlson, *Phenomenological model of a magnetorheological damper*, ASCE J. Eng. Mech. 123(3) (2003), pp. 230–238.
- [55] C.L. Giliomee and P.S. Els, *Semi-active hydro pneumatic spring and damper system*, J. Terramech. 35(2) (1998), pp. 109–117.

- [56] D. Sammier, O. Sename, and L. Dugard, *Skyhook and H_∞ control of semi-active suspensions: Some practical aspects*, Veh. Syst. Dyn. 39(4) (2003), pp. 279–308.
- [57] S.M. Savaresi, *The role of real-time communication for distributed or centralized architectures in vehicle dynamics control systems*, 6th IEEE International Workshop on Factory Communication Systems (WFCS 2006), Torino, Italy (plenary presentation), 2006, pp. 1–6.
- [58] E. Valtolina, S.M. Savaresi, S. Bittanti, A. Visconti, and A. Longhi, *A co-ordinate approach for the control of road vehicles*, 6th European Control Conference, Porto, Portugal, 2001, pp. 629–634.
- [59] I. Ballo, *Comparison of the properties of active and semiactive suspension*, Veh. Syst. Dyn. 45(11) (2007), pp. 1065–1073.
- [60] J. Wang and S. Shen, *Integrated vehicle ride and roll control via active suspensions*, Veh. Syst. Dyn. 46(1) (2008), pp. 495–508.
- [61] C. Poussot-Vassal, O. Sename, L. Dugard, P. Gaspar, Z. Szabo, and J. Bokor, *A new semi-active suspension control strategy through LPV technique*, Control Eng. Pract. 16(12) (2008), pp. 1519–1534.
- [62] M. Ahmadiam, B. Reichert, X. Song, and S.S. Southward, *No-jerk semi-active skyhook control method and apparatus*, US Patent 6.115.658, 2000.
- [63] K.H. Kahlil, *Nonlinear Systems*, 3rd ed., Prentice Hall, Upper Saddle River, NJ, 2002.
- [64] S.P. Boyd, L. El Ghaoui, E. Feron, and V. Balakrishnan, *Linear Matrix Inequality in Systems and Control Theory*, SIAM, Philadelphia, 1994.
- [65] D. Liberzon, *Switching in Systems and Control*, Birkhauser, Boston, MA, 2003.
- [66] D.E. Ivers and St K.A. Clair, *Adaptive off-state control method*, US Patent 6.311.110, 2001.